Ultrasonics Sonochemistry 76 (2021) 105617

Contents lists available at ScienceDirect

Ultrasonics Sonochemistry

journal homepage: www.elsevier.com/locate/ultson

Characterization of sonochemically prepared human serum albumin nanocapsules using different plant oils as core component for targeted drug delivery

Katharina Skoll, Matthias Ritschka, Stefanie Fuchs, Michael Wirth, Franz Gabor *

University of Vienna, Faculty of Life Sciences, Department of Pharmaceutical Technology and Biopharmaceutics, Althanstraße 14, 1090 Vienna, Austria

ARTICLE INFO

Keywords:
Targeted drug delivery
Human serum albumin
Proteinaceous nanocapsules
Sonochemical preparation

ABSTRACT

The focus of this study is the preparation of proteinaceous human serum albumin (HSA) nanocapsules with biocompatible plant oil cores avoiding toxic cross-linker and noxious non-aqueous liquids. The sonochemical preparation of HSA capsules with different plant oils yields particles with narrow size distribution forming suspensions stable for at least 14 days and enabling long-term storage by freezing. Furthermore, wheat germ agglutinin (WGA) as a targeting molecule was successfully embedded into the proteinaceous particle shell at a molar ratio of 7:1 (HSA/WGA). As urothelial cell binding studies revealed up to 55% higher cell binding potential of WGA-grafted particles than those without a targeter, targeted protein nanocapsules represent the first step towards new and innovative formulations.

1. Introduction

Protein particles offer, encompass a wide range of biomedical applications, including their use as contrast agents for myocardial echocardiography [1,2] and for magnetic resonance imaging [3], for contrast enhancement in electron paramagnetic resonance spectroscopy [4,5], and as drug delivery vehicles [6]. Nanoparticles in a narrow sense can be distinguished between nanospheres, in which the API (active pharmaceutical ingredient) is embedded in the particle matrix, and nanocapsules (NC's), where the protein forms a shell around solid or liquid API. [7] (Scheme 1)

Encapsulation of an API within a macromolecular drug delivery system reduces the passive diffusion of the drug into highly circulated tissue, which leads to lower toxicity and a reduced volume of distribution [11]. Lipophilic drugs with low bioavailability and thus limited therapeutic efficacy are particularly suitable for those carriers [12]. Especially drug delivery systems made from albumin are versatile macromolecular carriers because albumin is biodegradable, often non immunogenic and, compared to nanoparticles made of synthetic polymers, the clearance of albumin particles from the bloodstream by the reticuloendothelial system (RES) is slowed down. [13,14] Another benefit of albumin it is a well-established and well-studied excipient in vaccine formulation such as FSME Immun® and it is also used as a natural polymer for NPs in the chemotherapeutic formulation Abraxane®. As an additional utility to its functionality of transporting lipophilic drugs, it was reported that albumin accumulates in solid tumors, rendering it a suitable carrier for cancer drug delivery. [14,15]

Suslick et al. [16] developed a sonochemical method to produce gas- or liquid filled particles from various kinds of proteins such as bovine serum albumin (BSA) [16] and HSA [2]. They stated that the shell of the capsules is stabilized by disulfide bonds between the protein molecules. Radicals and superoxide, which are sonochemically produced by acoustic cavitation, are essential for this protein cross-linking. [17] The protein shell of the capsules, which is responsible for the high biocompatibility, has an average thickness of 50 nm and the core contains a non-aqueous liquid [18]. For the production of these proteinaceous NCs usually toxic water-immiscible liquids like n-dodecane, n-hexane, cyclohexane and mesitylene were used. [12,16] But to establish a vehicle appropriate for drug delivery a non-toxic lipophilic inner core is a crucial prerequisite e.g. made from plant oils.

To mediate active targeting properties to the capsules, plant lectins were so far used for surface modification of polylactide-co-glycolide (PLGA) nano- and microparticles [19,20]. Plant lectins bind to certain carbohydrate structures of the cell membrane and thus can trigger biochemical processes [21]. The lectin wheat germ agglutinin (WGA) possesses high affinity for urothelial cancer cells due to its specific

* Corresponding author.
E-mail addresses: katharina.skoll@univie.ac.at (K. Skoll), michael.wirth@univie.ac.at (M. Wirth), franz.gabor@univie.ac.at (F. Gabor).

https://doi.org/10.1016/j.ultsonch.2021.105617
Received 25 August 2020; Received in revised form 19 May 2021; Accepted 30 May 2021
Available online 4 June 2021

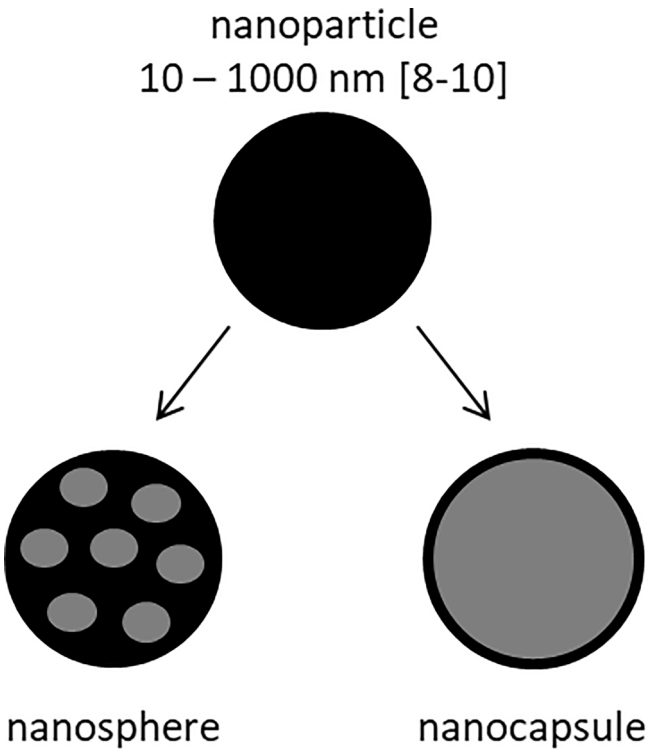

Scheme 1. Differentiation of nanoparticles in nanospheres and nanocapsules [8–10].

interaction with N-acetyl-D-glucosamine and sialic acid [22]. In addition the specificity of the WGA-cell interaction was previously shown under competitive inhibition with N,N′,N″-triacetylchitotriose, a complementary carbohydrate of high affinity to WGA [23–25]. Furthermore, binding of WGA to sugar moieties of the EGF receptor leads to a receptor-mediated endocytosis followed by internalization of the lectin and enrichment in lysosomal compartments [26].

As it was reported that the protein molecules building up the particle shell are scarcely denaturated during sonication process and thus their functional properties are maintained, glycotargeting of particles might be accomplished by using WGA as an additional proteinaceous component of the shell material [27]. That way, uptake of the incorporated drug into the cell might be promoted by receptor-mediated endocytosis of WGA.

In the present study, we aimed to develop WGA/HSA NCs as a targeted drug delivery system based on exploiting the glycotargeting properties of WGA. Here, we focused on the preparation of proteinaceous NCs with a narrow size distribution and aimed to ensure biocompatibility by using various plant oils as the core component. An additional focus was to establish a protocol for the production of proteinaceous NCs with different sizes depending on the oil used, to load the capsules with a lipophilic fluorescent dye as a model drug and to demonstrate the targeting effect of the WGA/HSA particles.

2. Materials and methods

2.1. Chemicals

Wheat germ agglutinin (WGA) from *Triticum Vulgare* was purchased from Vector laboratories (Burlingame, CA, USA) and HOECHST 33342 from Invitrogen (Paisley, UK). Human serum albumin (HSA), cottonseed oil, Kolliphor® P188 (KP188) and the cell culture medium RPMI-1640 were obtained from Sigma-Aldrich (St. Louis, MO, USA). BodiPy® 493/503 (BodiPy®) was bought from Invitrogen (Eugene, Oregon, USA). n-Dodecane, olive oil, almond oil, rapeseed oil and linseed oil were purchased from Carl Roth GmbH & Co. KG (Karlsruhe, Germany). All other chemicals used were obtained from Carl Roth GmbH & Co. KG (Karlsruhe, Germany) or Sigma Aldrich (Seelze, Germany).

2.2. Sonochemical preparation of HSA/WGA NCs

In this study, a protocol using n-dodecane as a lipophilic phase was optimized [28]. For the preparation of NC with oil as core component, different plant oils were heated up to 40 °C and subsequently 1 ml layered over 10 ml of 2% (w/v) aqueous HSA solution or a WGA/HSA (1 + 2) 2% (w/v) solution. The ultrasonic micro-tip connected to a Bandelin HD 2070 sonifier was positioned at the interface of the two phases; the sample was sonicated with an acoustic power of ≈253 W cm^{-2} at 40% amplitude for 2 min. Afterwards, NCs were purified by centrifugation (5204×*g*, 40 min and 4 °C), discarding the supernatant and dispersing the floating pellet in 1% (w/v) Kolliphor® P188 (KP188). A separation flask was used to achieve a complete separation of the capsules from the non-encapsulated oil within 12 h at room temperature. The residual aqueous phase containing the capsules was used for further experiments.

Fluorescence-labelled NCs were prepared as described above, however BodiPy®, a fluorescent dye used as a lipophilic model drug, was added to the plant oil after dissolution 1 mg in 500 µl dichlormethane which was used as solubilizing agent. Before sonication dichlormethane was cleared off.

2.3. Characterization of the proteinaceous NCs

Size and polydispersity index (PDI) were acquired by laser light scattering (Zetasizer Nano ZS, Malvern Panalytical, Malvern, UK). The morphology of the protein capsules was disclosed by cryo-transmission electron microscopy. Therefore, four µl sample aliquots were applied to Quantifoil (Großlöbichau, Germany) Cu 200 mesh R3.5/1 holy carbon grids loaded into a Leica GP (Leica Microsystems, Vienna, Austria) grid plunger. Grids were blotted for 2–4 s and plunge frozen into liquid ethane for instant vitrification. Cryo-samples were analyzed at a Glacios cryo-transmission microscope (Thermo Scientific, USA) equipped with a X-FEG and images were recorded at 200 kV in low-dose mode using the SerialEM software (Mastronarde, 2005) with a Falcon3 direct electron detector in low dose mode at a magnification of 28,000 and a pixel size of 5.19 Å.

Furthermore, to quantify the amount of WGA encapsulated in the shell a fluorescence-labelled WGA was used for production of NC's. The quantity of encapsulated targeting molecule was analyzed after resumption of the lyophilisate in 500 µl distilled water using a fluorimeter at 485/525 ex/em.

Furthermore, to estimate the WGA-content in the shell of the particles, NC's were prepared using the fluorescein-labelled analogue. The lyophilized NC's were dispersed in 500 µl distilled water and the quantum yield was determined at 485/525 nm (ex/em).

In order to detect alterations of the surface characteristics of the shell due to immobilization of the targeter, the number of free amino-groups was determined by mixing 200 µl particle suspension with 50 µl Fluoraldehyde™ amino assay reagent and measuring the fluorescence intensity at 360/455 nm (exc/em) after incubation for 5 min. The assay was calibrated with 1,4-diaminobutane.

In addition, to investigate if the incorporated targeter molecule has any effects on the surface condition of the particles, free amino-groups of the capsules were analyzed using 50 µl Fluoraldehyde™ amino assay reagent in a 96-well plate with 200 µl particle suspension following the measurement of the fluorescence at 360 nm/455 nm (exc/em). The amount of free amino groups was specified using a calibration curve with 1,4-diaminobutane.

2.4. Stability studies and freeze-thaw experiments

The stability of the NCs was tested at room temperature and at 4 °C over a period of 14 days using dynamic light scattering (DLS). In order to elucidate the behavior of NC under several storage conditions, different freezing procedures (-20 °C, −80 °C and liquid nitrogen) were applied. After gently thawing at room temperature, the average size of the NC's was determined.

2.5. Viscosity measurements

Rheological parameters of the oils used were collected on a MCR Modular Compact Rheometer 302 (Anton Paar, Graz) equipped with a thermostatic control system and a cone-and-plate measuring system (diameter: 25 mm; cone angle: 2°). The temperature was maintained at 40 °C ± 0.2 °C throughout all measurements to mimic the temperature used for the preparation of the particles. To describe the flow behavior of the oil, the dynamic viscosity η (in Pa·s) was determined while increasing the shear stress. A shear rate ranging from 1 to 100 s^{-1} was applied and the plant oils were compared at a shear rate of 100 s^{-1}.

2.6. Interaction of the NCs with urothelial cancer cells

2.6.1. Cell culture

The interaction between the NC and the cell surface was assessed using 5637 cells, a cell line established from a grade 2 human urothelial carcinoma (ATCC, Rockville, MD, USA).

Cells were cultivated at 37 °C in a humidified 5% CO_2/95% air atmosphere in RPMI-1640 supplemented with 10% fetal calf serum (Sigma Aldrich, St. Louis, MO, USA), antibiotics and 0.5 mM L-glutamine. 5637 cells were subcultivated at about 80% confluency by trypsination and used for binding and internalization studies between passages 40 and 65.

2.6.2. Urothelial cell binding

Surface binding as well as a potential uptake of the particles were examined using 5637 single cells and monolayers.

For single cell binding studies, cells were subcultivated using 0.25% trypsin/0.038% EDTA and adjusted to a cell count of 6×10^6 cells per ml. 50 µl of the pre-cooled cell suspension were incubated with 50 µl particle suspension (corresponding to 2.88 µg/ml, 1.44 µg/ml and 0.72 µg/ml BodiPy®) for 30 min at 4 °C to limit active transport into the cytosol. Afterwards, the supernatant was redispersed in 900 µl cold 3 mM phosphate buffered saline supplemented with Ca^{+2} and Mg^{+2} (PBS) and the amount of cell-bound capsules was assessed at 488/525 nm (ex/em) using flow cytometry (Gallios, Beckmann Coulter, Brea, USA).

For monolayer studies cells were seeded at a density 1.7×10^4 per well in 96-well microplates (Greiner Bio-One, Frickenhausen, Germany) or on microscope slides mounted with flexiPERM® (Greiner Bio-one, Frickenhausen, Germany) and grown to confluency. Initially, the monolayer was washed with cold PBS followed by 30 min incubation at 4 °C with 50 µl particle suspension or 50 µl PBS as a negative control. The particle suspensions were adjusted to a BodiPy® content of 2.88 µg/ml, 1.44 µg/ml or 0.72 µg/ml according to their fluorescence intensity finally corresponding to the resulting concentrations of 0.56 mg/ml, 0.28 mg/ml and 0.14 mg/ml particles. After the incubation, unbound particles were removed by careful aspiration of the supernatant and three washes with 100 µl of cold PBS. The cell associated relative fluorescence intensity (RFI) was determined at 485/525 nm (ex/em) using a microplate reader (Infinite M200 Pro fluorometer, TECAN, Grödig, Austria).

For colocalization studies, single cells and monolayers were incubated as described above. To elucidate localization of the particles, the cell membrane and the nucleus were stained using fluorescent labelled Alexa–WGA (aWGA) with a final concentration of 24 µg/ml and the DNA-specific fluorescent dye HOECHST 33,342 (final concentration 36 µg/ml), respectively. To prevent internalization of the particles into the cytosol, cells were fixed for 10 min at 4 °C with 2% paraformaldehyde in PBS. To inactivate non-reacted paraformaldehyde, ammonium chloride was added up to a final concentration of 50 mM and subsequent incubation for 10 min at room temperature. After the staining and several washing steps, colocalization was assessed using a Zeiss Epifluorescence Axio Observer. Z1 deconvolution microscopy system (Carl Zeiss, Oberkochen, Germany).

To detect potential internalization of the particles, cells were incubated with the same amounts of capsules and HOECHST 33342 as above but for 30 min at 37 °C. Prior to membrane staining, cells were cooled to 4 °C and, after staining the cell membrane with aWGA, they were washed and fixed as described above.

2.7. Statistics

All data are presented as mean ± standard deviation (SD) of at least three independent measurements. Comparisons between groups were calculated using Mann-Whitney Rank Sum Test and Welch's Test; p-values ≤ 0.05 (*) were considered statistically significant, p-values ≥ 0.05 (n.s.) show that there is no significant difference between the compared groups. SigmaPlot 13 software (Systat Software, Inc., San Jose, CA, USA) was used for calculations.

3. Results and discussion

In this study, we aimed to develop protein particles featuring three key characteristics: They should be nano-sized, toxic ingredients should be avoided and they should possess cell-associative properties due to targeting molecules in the shell of the capsule. This manufacturing technology avoids the use of chemicals for cross-linking or hazardous non-aqueous liquids as core components. Instead of glutaraldehyde as a commonly used for cross-linker for proteins ultrasound is applied to yield particles. During sonication a perhydroxyl radical is generated that oxidizes cysteine residues of the protein chains to yield disulfide bridges and finally a protein network around an oily core [2]. Thus, the resulting NCs entrap plant oil instead of toxic non-aqueous solvents. Since further studies [27] showed that the protein in the particle shell is not significantly denatured during sonication and retains important functional properties it is expected that the targeting characteristics of WGA are still retained as well.

3.1. Preparation of HSA nanocapsules with different plant oils and their characteristics

Adhering to the protocol described above monodisperse (PDI < 0.2) proteinaceous NCs were successfully prepared. The size of the capsules is mainly determined by the type of oil used as an inner phase. Rapeseed oil yielded the largest NCs (862.2 ± 59.5 nm). Slightly smaller capsules (835.8 ± 70.4 nm) were produced with olive oil. Applying linseed oil, cotton seed oil and almond oil, resulted in NCs with small alteration of size (760.4 ± 79.3 nm, 709.4 ± 80.4 nm and 816.4 ± 95.6 nm, respectively). Capsules generated using n-dodecane were smaller (655.0 ± 27.4 nm) as compared to the plant oils investigated. Particles with WGA/HSA as a shell component and olive oil as a core component had a slightly smaller diameter (662.1 ± 7.6 nm) as compared to the HSA particles with olive oil as core. To evaluate whether the viscosity of the oil exerts an impact on the size of the particles rheological measurements were conducted (Table 1).

The values acquired at a shear rate of 100 s^{-1} ranged from 38 to 59 mPa·s for the plant oils tested and covered a wide viscosity range. Thus, plant oils are complex mixtures of glycerides, fatty acids, phospholipids and other components [30,31] with varying viscosities, nourishing the hypothesis that complex interactions of these properties are responsible for the different sizes of the particles. In this work we produced NCs with oil as core component in a size range from 655 nm to 862 nm with a

Table 1
Dynamic viscosity (η) of plant oils determined at 40 °C (mean ± SD, n = 12). The viscosity of n-dodecane was taken from literature because it was not able to measure the viscosity with the same parameters used for the oils.

Plant oil	η [mPa•s]	Size	PDI
n-dodecane	0.91 (50 °C) [29]	655.0 ± 27.4	0.11 ± 0.02
Olive oil	43.0 ± 0.5	835.8 ± 70.4	0.17 ± 0.05
Linseed oil	29.0 ± 0.5	760.4 ± 79.3	0.30 ± 0.06
Cotton seed oil	59.0 ± 1.0	709.4 ± 80.4	0.21 ± 0.06
Almond oil	41.0 ± 0.1	816.4 ± 95.6	0.18 ± 0.06
Rapeseed oil	38.0 ± 1.0	862.2 ± 59.5	0.24 ± 0.08

narrow size distribution.

To confirm alterations in surface characteristics due to entrapment of the targeter, the number of amino-groups served as a measure. When the particles were prepared without WGA, 9.5 ± 0.01 μmol free amino-groups per mg capsules were detected. In presence of WGA, however, the number of amino groups decreased by a third amounting to 6.09 ± 0.112 μmol/mg particles. Thus, a considerable number of free accessible amino-groups of HSA are shielded due to inclusion of targeting molecules. To get a closer idea of the WGA-density on the surface of the NC's, a fluorescein-labelled analogue (f-WGA) of the targeter was used for manufacturing of the delivery devices. Reading the fluorescence intensity revealed that 0.63 ± 0.03 mg capsules contained 0.046 ± 0.001 mg f-WGA corresponding to targeting molecule content of about 7%. Due to the quite different molecular weight between HSA and WGA, their molar ratio matrix and targeting molecules is 7:1.

The morphology of the NCs was visualized by cryo-TEM imaging and confirms the spherical shape (Fig. 1). Most probably due to the sample preparation method for cryo-TEM imaging, the measured diameter of HSA NCs with n-dodecane core is slightly smaller than the mean size of the capsules determined by dynamic laser light scattering.

3.2. Storage stability

Apart from preparation of NCs in a reproducible manner, storage stability of the nano-formulation is a prerequisite for any application. For that purpose, the NCs were stored for two weeks at room temperature and at 4 °C. According to DLS measurements, the particle suspensions made with olive oil, rapeseed oil, almond oil and linseed oil can be stored for at least 14 days at 4 °C as well as at room temperature without any change in size ($p > 0.05$) (Fig. 2). The diameter of the particles prepared with cotton seed oil did not significantly change until day eight ($p > 0.05$). Thereafter, it significantly decreased ($p < 0.05$) at both temperature levels. The size of particles made with n-dodecane significantly ($p < 0.05$) increased due to aggregation and it is not possible to store a suspension, neither at 4 °C nor at room temperature (Fig. 2).

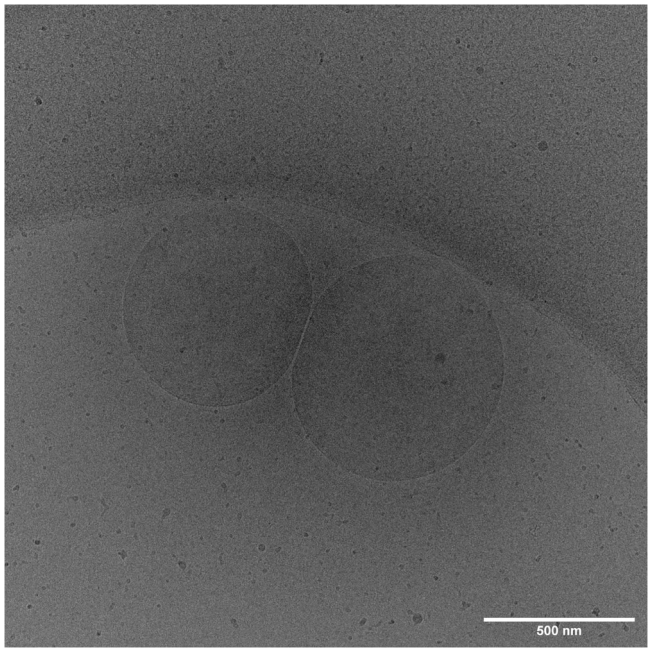

Fig. 1. Cryo-TEM micrograph of proteinaceous NCs filled with n-dodecane.

Slight differences were observed in the mean zeta potentials of particles prepared with olive oil (−12.3 ± 3.2 mV), almond oil (−14.8 ± 2.7 mV) and rapeseed oil (−12.4 ± 9.4 mV). On average the zeta potential of the mentioned NCs was around −13.17 mV. Capsules made with cotton seed oil and linseed oil showed a considerably more positive zeta potential (−4.8 ± 0.5 mV and −1.2 ± 1.4 mV, respectively). As a rule of thumb, a zeta potential exceeding ± 30 mV is an indicator for electrostatic stabilization of a nano-suspension [32]. Considering the results of our experiments, however, no significant aggregation of the particles made with plant oils occurred over a period of at least eight days both at 4 °C and at room temperature. To complete the stability testing, also the PDI was examined over a period of 14 days. Comparison of the initial PDI of particles made from olive oil, rapeseed oil, almond oil and linseed oil with those determined at day 8 and day 14 revealed no significant ($p > 0.05$) changes. The PDI of particles produced with cotton seed oil are comparable with the size measurements, until day 8 the PDI did not significantly ($p > 0.05$) changed. Afterwards the PDI significantly ($p < 0.05$) increased at the same time as the size measurements also showed a significant change. Independent of storage temperature the size as well as the PDI of n-dodecane particles continuously and significantly ($p < 0.05$) increased over 14 days indicating agglomeration and thus instability of the formulation (Fig. 2).

To examine their long-term storage stability the NCs were frozen at different temperatures and after a gentle thawing process the particle size was determined by DLS. Storage of particles at subzero temperatures should mitigate potential risks associated with aggregation. After freezing at −20 °C, the size as well as the PDI of nearly all particle suspensions increased. Freezing the particles at −80 °C did hardly change the particle size as compared to the initial values in case of olive oil and almond oil as an inner phase (Table 2). Upon long-term storage at temperatures below −20 °C, NCs produced with n-dodecane, rapeseed oil, olive oil as well as almond oil showed no considerable alteration in particle size. The experiments also revealed that the size of olive oil particles and almond oil particles did not significantly increase by freezing neither at −80 °C nor at −196 °C in liquid nitrogen. Similarly, rapeseed oil and n-dodecane particles are storable in liquid nitrogen with no significant increase in size. The results further showed that freezing the suspension at −20 °C leads to growth of all particle preparations, which is due to aggregation of the proteinaceous capsules. Furthermore, it was observed that particles prepared with linseed oil and cotton seed oil cannot be stored frozen without significant particle aggregation. Due to their advantages in terms of zeta potential, mid-range size (835.8 ± 70.4 nm), the good stability in suspension as well as the benefit of long-term storage via freezing, capsules made with olive oil were used for further cell experiments.

3.3. Cell studies

To confer the cell-associative properties of WGA to the NCs, the lectin was incorporated as a targeter into the protein shell. That way, targeted and non-targeted particles were manufactured and their cytoadhesive potential was compared.

To assess the targeting effect of the WGA/HSA capsules via the lectin domain, 5637 single cells were incubated with plain and WGA-grafted HSA NCs, respectively. The particle suspensions were labelled by incorporation of the fluorescent dye BodiPy®. For comparability of data, particles with and without targeting moiety were adjusted to the same

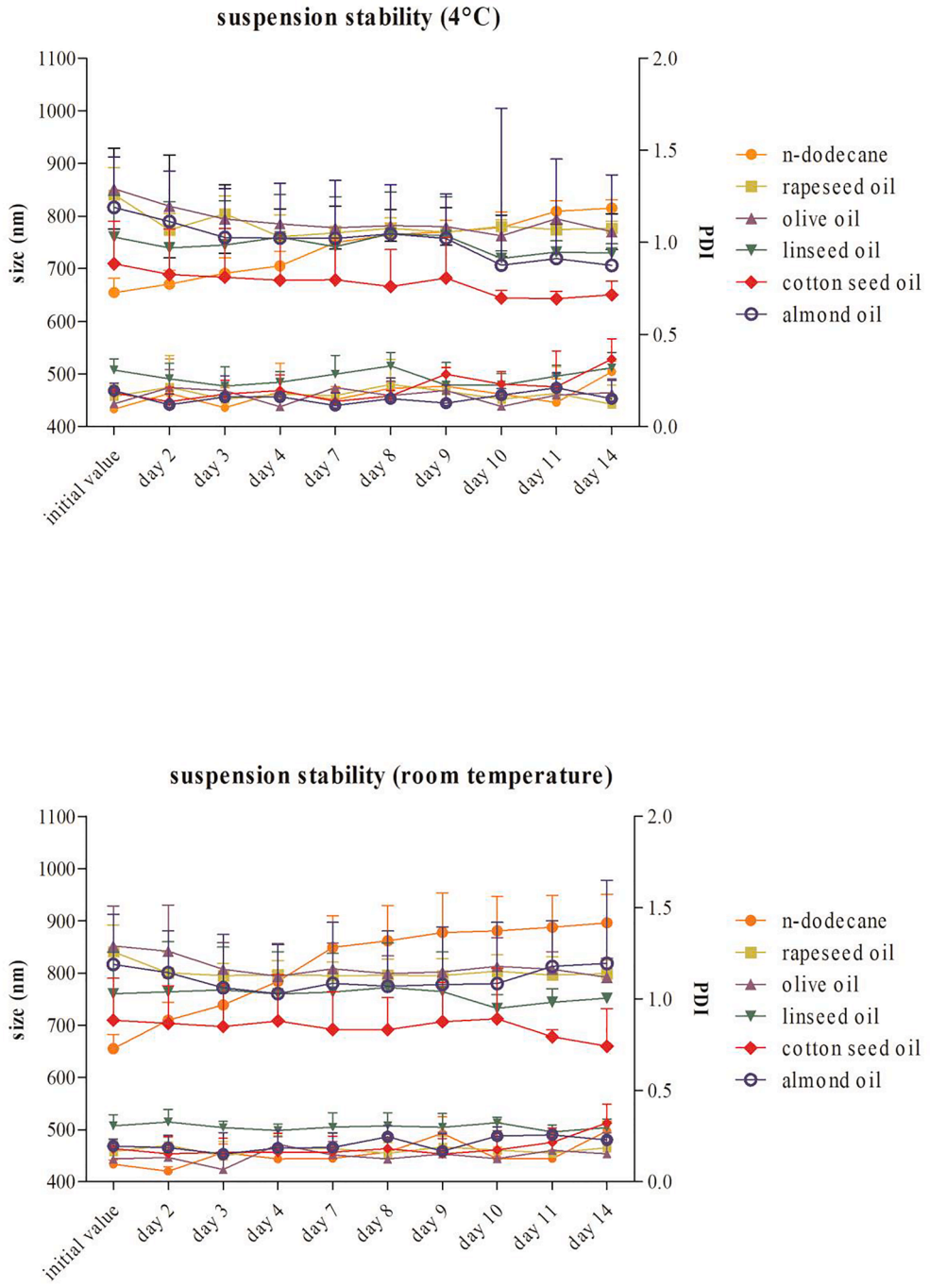

Fig. 2. The diameter (upper graph) and PDI (lower graph) of HSA-NCs prepared with different lipophilic phases after storage at 4 °C (A) and at room temperature (B). For p-values the sizes at day 4, at day 8 and at day 14 were compared to the initial size of the particles.

fluorescence intensity. The initial WGA/HSA particle suspension (2.88 μg/ml BodiPy®) – and for comparison also the HSA particle suspension – was diluted to 1.44 μg and 0.72 μg BodiPy® per ml particle suspension. Single cell-association was determined by flow cytometry and monolayer association by reading the cell-associated fluorescence intensity at 488/525 nm (ex/em).

In order to minimize energy consuming transport processes and to reduce fluidity of the cell membrane the assay was performed at 4 °C. Thus, mainly binding of the NCs to the cell membrane and not uptake is investigated. Monitoring the cell-associated relative fluorescence intensity (RFI) revealed that the amount of cell-bound NCs concurrently increased with concentration of NCs independent from surface modification of the HSA-NCs (Fig. 3). However, regarding the extent of cell-binding, the specific interaction between WGA-grafted HSA-NCs and cells exceeded the non-specific interaction between plain HSA-NCs and cells. Although plain HSA-NCs possess a high inherent cell-binding capacity that even withstands the shear forces during flow cytometry, grafting their surface with the bioadhesive lectin increases the cell-binding by 55% (2.88 μg/ml), 37% (1.44 μg/ml) and 28% (0.72 μg/ml BodiPy®) at the mean.

The highest cell-associated RFI (19.23 ± 0.49) was measured for the WGA/HSA capsules with the highest concentration of BodiPy® (2.88 μg/ml) decreasing to an RFI of 9.63 ± 0.28 (1.44 μg/ml BodiPy®) and 6.43 ± 0.18 (0.72 μg/ml BodiPy®), respectively. Compared to the capsules with targeting moiety, the particles without WGA showed a significantly lower cell-association. The RFI, however, also decreased in

Table 2
Hydrodynamic diameter of NCs produced with different oils after freezing/thawing. For p-values the initial size and the size of the thawed particles were compared.

	n-Dodecane		Rapeseed oil		Olive oil		Linseed oil		Cotton seed oil		Almond oil	
	Size average [nm]	PDI	Size average [nm]	PDI	Size average [nm]	PDI	Size average [nm]	PDI	Size average [nm]	PDI	Size average [nm]	PDI
Initial size	655.0 ± 27.4	0.11 ± 0.02	862.2 ± 59.5	0.24 ± 0.08	835.8 ± 70.4	0.17 ± 0.05	760.4 ± 79.3	0.30 ± 0.06	709.4 ± 80.4	0.21 ± 0.06	816.4 ± 95.6	0.18 ± 0.06
Liquid nitrogen	673.7 ± 22.3$^{n.s.}$	0,1 ± 0.02	903.3 ± 139.7$^{n.s.}$	0.22 ± 0.08	856.4 ± 69.9$^{n.s.}$	0.12 ± 0.05	1098.3 ± 178.1 *	0.32 ± 0.04	998.5 ± 59.6 *	0.24 ± 0.02	814.6 ± 121.4$^{n.s.}$	0.21 ± 0.12
−80 °C	722.1 ± 16.3 *	0.21 ± 0.03	1005.9 ± 182.4 *	0.29 ± 0.05	891.3 ± 8.4$^{n.s.}$	0.22 ± 0.09	1984.3 ± 414.0 *	0.14 ± 0.06	972.5 ± 69.6 **	0.26 ± 0.04	896.9 ± 155.1$^{n.s.}$	0.34 ± 0.09
−20 °C	852.2 ± 9.2 *	0.18 ± 0.04	2374.0 ± 592.9 *	0.45 ± 0.31	2500.0 ± 1336.1 *	0.52 ± 0.07	2032.0 ± 1320.3 *	0.94 ± 0.10	1782.9 ± 1019.4 *	0.81 ± 0.04	3119.0 ± 3005.2 *	0.51 ± 0.06

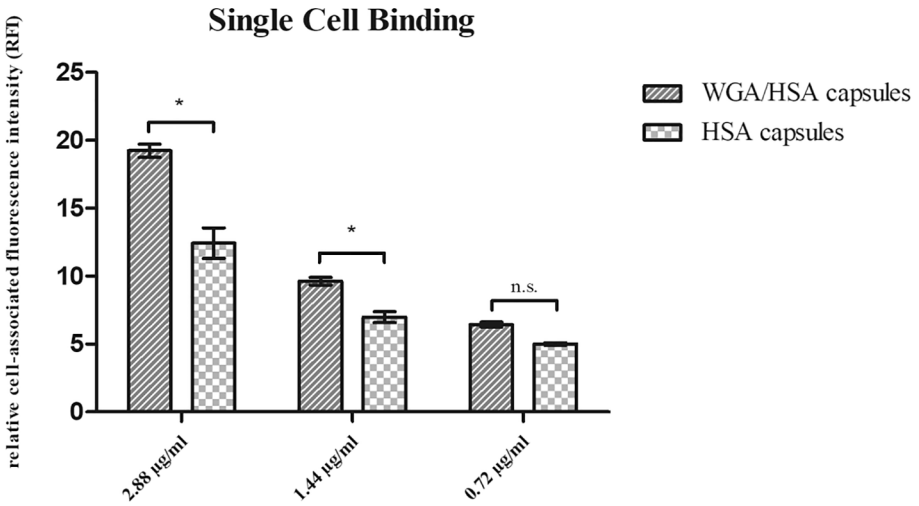

Fig. 3. Cell surface binding of olive oil particles with and without WGA targeting molecule at urothelial 5637 single cells. For comparability, particle suspensions were adjusted to 2.88 µg, 1.44 µg and 0.72 µg BodiPy® and cell-association was determined at 488/525 nm (ex/em) (Mean ± SD, n = 3).

case of that particle suspensions with decreasing concentrations of BodiPy® from 12.43 ± 1.13 (2.88 µg/ml) to 6.98 ± 0.40 (1.44 µg/ml) and 5.0 ± 0.01 (0.72 µg/ml BodiPy®) (Fig. 3). Differences between capsules with and without targeting molecule were statistically significant for higher concentrations. A small amount of protein particles without a targeting molecule bound via non-specific protein interactions to the cell surface compared to the capsules with WGA, which showed a 1.5-fold higher cell-associated RFI. At the lowest concentration of BodiPy® no significant difference between the non-specific proteinaceous interaction and the specific interaction via WGA could be detected.

Binding characteristics depending on the target component WGA were also assessed on monolayers to confirm the previously shown concentration-dependent interaction of the capsules with the cells. The cell-associated fluorescence intensity of bound WGA/HSA capsules

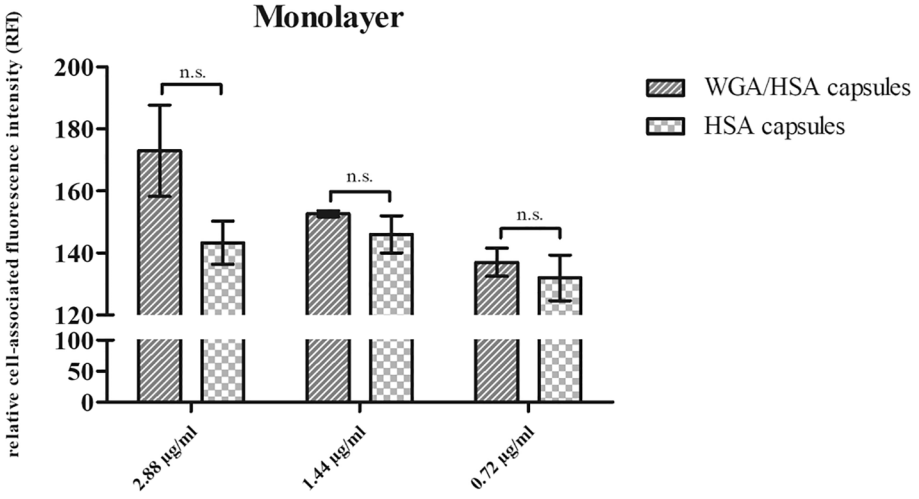

Fig. 4. Interaction of targeted and non-targeted particles with 5637 cell monolayers. For comparability the particle suspensions were adjusted to the same concentrations of BodiPy® (2.88 µg/ml, 1.44 µg/ml and 0.72 µg/ml) as used in single cell experiments (Mean ± SD, n = 3).

increased from 137.00 ± 4.54 via 152.67 ± 1.00 to 173.00 ± 14.72 corresponding to the amount of particles specifically interacting with the cell glycocalyx (Fig. 4). Considering the amount of NCs added, the RFI of the capsules without targeting moiety did not vary significantly from 132.00 ± 7.35 (0.72 μg/ml BodiPy®) to 146.00 ± 6.00 (1.44 μg/ml BodiPy®) and 143.33 ± 6.94 (2.88 μg/ml BodiPy®). Thus, a tendency for the interaction of HSA capsules with cells could not be observed within the concentration range tested (Fig. 4). In contrast, the cell-binding potential of HSA/WGA capsules was 1.2-fold higher than that of targeter–free NCs (2.88 μg/ml BodiPy®), which is comparable to the single cell results. Again, at lower concentrations (0.72 μg/ml BodiPy® and 1.44 μg/ml BodiPy®) the binding potential of targeter-grafted NCs was higher at the mean although being not significant. Obviously, floating of the oily capsules and thus timely limited duration of the monolayer – capsule interaction contributes to low significance.

3.4. Colocalization analysis

To examine and discriminate between the cytoadhesive potential due to protein as well as lectin and the cytoinvasive potential mediated by the lectin colocalization studies were performed using human urothelial 5637 single cells as well as monolayers. In general, nano-sized protein particles offer certain advantages in-vivo: they can deeply penetrate into tissues through fine capillaries and are generally taken up efficiently by the cells [33].

When the cells were incubated with plain HSA-NCs at 4 °C (Fig. 5B) a lonesome green NC is associated with the cell membrane stained in red. In contrast, grafting the surface with bioadhesive lectin results in accumulation of a lot of NCs within the cell membrane (Fig. 5A). Raising the temperature to 37 °C and thus allowing energy consuming transport processes like endocytosis yielded quite different images: In case of non-grafted HSA-NCs a few green NCs with low fluorescence intensity are observed within membrane regions. There are weak green irradiation points in the area of the blue nucleus which appear to be inside the cells. Most probably, however, they are due to a crossover effect deriving from strongly fluorescent NCs out of plane at the cell membrane (Fig. 5B, 37 °C). In case of WGA-grafted HSA-NCs a high number of strongly fluorescent the green particles accumulate within the red stained cell membrane around the blue nucleus in the cytoplasm (Fig. 5A, 37 °C).

According to studies with WGA [26], this lectin is internalized and enriched in lysosomal compartments due to its binding to the sugar structures of the EGF receptor, which induces a receptor-mediated endocytosis, suggesting that WGA can transfer its cytoadhesive and cytoinvasive characteristics to bigger particles like HSA-NCs in a piggyback manner. Furthermore, this principle also works in artificial urothelial tissue as confirmed by images of cell monolayers incubated

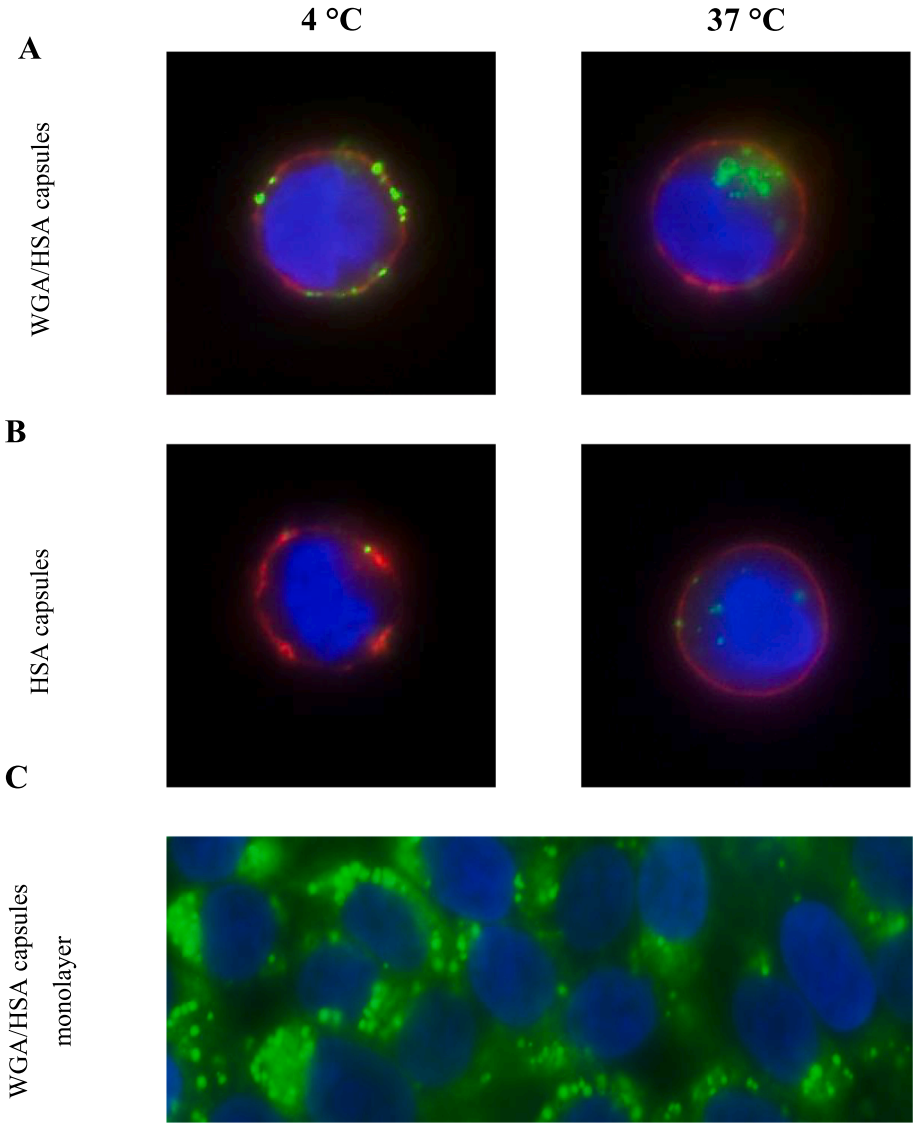

Fig. 5. Microscopic analysis of the interaction between WGA/HSA-NCs and HSA-NCs with human urothelial 5637 cells. Interaction of WGA/HSA particles with single cells at 4 °C and at 37 °C one cell was selected which represents the entire cells observed (**A**) Interaction of HSA capsules with single cells as well at 4 °C and at 37 °C (**B**) Interaction of WGA/HSA particles with confluent cell monolayers at 37 °C (**C**). (Nucleus blue, cell membrane red, NCs green). (For interpretation of the references to colour in this figure legend, the reader is referred to the web version of this article.)

with WGA/HSA-NCs at 37 °C, where a high number of green particles are enriched around the blue nuclei of the tissue (Fig. 5C).

4. Conclusion

To the best of our knowledge, this is the very first publication which deals with the production of proteinaceous NCs with a narrow size distribution and different plant oils as core component. In particular, these NCs are manufactured avoiding toxic water-immiscible core components and/or toxic cross-linkers. Moreover, the NCs are stable and can be stored at 4 °C as well as at room temperature for at least two weeks. For long-term storage, they can be frozen at – 80 °C or in liquid nitrogen.

In addition, the NCs possess inherent non-specific bioadhesive characteristics most probably due to the proteinaceous shell. Nevertheless, the adhesion to cells can be further increased and even uptake into the cell can be mediated by coupling a targeter as confirmed by binding studies to urothelial cells. Due to the availability of carboxylate, amino and thiol-groups of the protein shell an array of different coupling techniques is available to increase functionality. Cell association studies as well as microscopic analyses revealed not only adhesion at the cell membrane, but also uptake into urothelial cells with a preference for cancer cells [22].

The WGA/HSA particles produced during this study might be useful for delivery of lipophilic therapeutic agents while targeting especially urothelial cancer cells. Because conventional therapeutic approaches for the treatment of non-muscle invasive bladder cancer has its shortcomings such as the high resistance of the bladder wall itself [34,35], keeping urothelial drug uptake, if at all, extremely low [36]. Additionally, dilution of the instilled drug solution, either with the continuously produced urine or residual urine in the bladder cavity, limits the therapeutic success. Moreover, the administrable instillation volume has to be considered, since a filling volume above 150 ml is rather inconvenient for the patient [37]. Therefore, WGA equipped particles could improve the treatment of bladder cancer by prolonging the druǵs residence time in the bladder cavity and/or by enhancing the permeation rate of the incorporated drug. Consequently, further investigations will focus on establishing a protocol for loading the NCs with lipophilic drugs and further elucidating the drug release characteristics.

This research did not receive any specific grant from funding agencies in the public, commercial, or not-for-profit sectors.

CRediT authorship contribution statement

Katharina Skoll: Conceptualization, Investigation, Methodology, Writing - original draft, Formal analysis. **Matthias Ritschka:** Data curation. **Stefanie Fuchs:** Data curation. **Michael Wirth:** Writing - review & editing. **Franz Gabor:** Supervision, Writing - review & editing.

Declaration of Competing Interest

The authors declare that they have no known competing financial interests or personal relationships that could have appeared to influence the work reported in this paper.

References

[1] M.W. Keller, S.S. Segal, S. Kaul, B. Duling, The behavior of sonicated albumin microbubbles within the microcirculation: A basis for their use during myocardial contrast echocardiography, Circ. Res. 65 (2) (1989) 458–467.
[2] M.W. Grinstaff, K.S. Suslick, Air-filled proteinaceous microbubbles: synthesis of an echo-contrast agent, Proc. Natl. Acad. Sci. U. S. A. 88 (17) (1991) 7708–7710.
[3] A.G. Webb, M. Wong, K.J. Kolbeck, R.L. Magin, K.S. Suslick, Sonochemically produced fluorocarbon microspheres: A new class of magnetic resonance imaging agent, J. Magn. Reson. Imaging 6 (4) (1996) 675–683.
[4] J.J. Eckburg, J.C. Chato, K.J. Liu, M.W. Grinstaff, H.M. Swartz, K.S. Suslick, F. P. Auteri, The measurement of temperature with electron paramagnetic resonance spectroscopy, J. Biomech. Eng. 118 (2) (1996) 193–200.
[5] K.J. Liu, M.W. Grinstaff, J. Jiang, K.S. Suslick, H.M. Swartz, W. Wang, In vivo measurement of oxygen concentration using sonochemically synthesized microspheres, Biophys. J. 67 (2) (1994) 896–901.
[6] A. Rollett, T. Reiter, P. Nogueira, M. Cardinale, A. Loureiro, A. Gomes, A. Cavaco-Paulo, A. Moreira, A.M. Carmo, G.M. Guebitz, Folic acid-functionalized human serum albumin nanocapsules for targeted drug delivery to chronically activated macrophages, Int. J. Pharm. 427 (2) (2012) 460–466.
[7] Alfred Fahr. Voigt's Pharmaceutical Technology, 2015. Pp. 456–458.
[8] P. Couvreur, P. Tulkenst, M. Roland, A. Trouet, P. Speiser, Nanocapsules: A new type of lysosomotropic carrier, FEBS Lett. 84 (2) (1977) 323–326.
[9] P. Couvreur, B. Kante, V. Lenaerts, V. Scailteur, M. Roland, P. Speiser, Tissue distribution of antitumor drugs associated with polyalkylcyanoacrylate nanoparticles, J. Pharm. Sci. [Internet] 69 (2) (1980) 199–202.
[10] P. Couvreur, B. Kante, M. Roland, P. Guiot, P. BAuduin, P. Speiser, Polycyanoacrylate nanocapsules as potential lysosomotropic carriers: preparation, morphological and sorptive properties. J. Pharm. Pharmacol. 31(1);(1979):331–2.
[11] O. Grinberg, A. Gedanken, C.R. Patra, S. Patra, P. Mukherjee, D. Mukhopadhyay, Sonochemically prepared BSA microspheres containing Gemcitabine, and their potential application in renal cancer therapeutics, Acta Biomater. 5 (8) (2009) 3031–3037.
[12] O. Grinberg, M. Hayun, B. Sredni, A. Gedanken, Characterization and activity of sonochemically-prepared BSA microspheres containing Taxol - An anticancer drug, Ultrason. Sonochem. 14 (5) (2007) 661–666.
[13] A.O. Elzoghby, W.M. Samy, N.A. Elgindy, Protein-based nanocarriers as promising drug and gene delivery systems, J. Control. Release 161 (1) (2012) 38–49.
[14] F. Kratz, I. Fichtner, U. Beyer, P. Schumacher, T. Roth, H.H. Fiebig, C. Unger, Antitumour activity of acid labile transferrin and albumin doxorubicin conjugates in in vitro and in vivo human tumour xenograft models, Eur. J. Cancer 33 (8) (1997) 175.
[15] Y. Matsumura, H. Maeda, A new concept for macromolecular therapeutics in cancer chemotherapy: mechanism of tumoritropic accumulation of proteins and the antitumor agent smancs, Cancer Res. 46 (8) (1986) 6387–6392.
[16] K.S. Suslick, M.W. Grinstaff, Protein microencapsulation of nonaqueous liquids, J. Am. Chem. Soc. [Internet] 112 (21) (1990) 7807–7809.
[17] M.W. Grinstaff, K.S. Suslick, Proteinaceous microsperes, Am. Chem. Soc. 493 (1992) 218–226.
[18] F.-J. Toublan, S. Boppart, K.S. Suslick, Tumor targeting by surface-modified protein microspheres, J. Am. Chem. Soc. 128 (11) (2006) 3472–3473.
[19] B. Brauner, C. Schuster, M. Wirth, F. Gabor, Trimethoprim-loaded microspheres prepared from low-molecular-weight PLGA as a potential drug delivery system for the treatment of urinary tract infections, ACS Omega 5 (15) (2020) 9013–9022.
[20] R. Wang, J. Huang, J. Chen, M. Yang, H. Wang, H. Qiao, Z. Chen, L. Hu, L. Di, J. Li, Enhanced anti-colon cancer efficacy of 5-fluorouracil by epigallocatechin-3- gallate co-loaded in wheat germ agglutinin-conjugated nanoparticles, Nanomed. Nanotechnol. Biol. Med. 21 (2019) 102068.
[21] I.J. Goldstein, C.E. Hayes, The lectins: carbohydrate-binding proteins of plants and animals, Adv. Carbohydr. Chem. Biochem. 35 (1978) 127–340.
[22] L. Neutsch, V.E. Plattner, S. Polster-Wildhofen, A. Zidar, A. Chott, G. Borchard, O. Zechner, F. Gabor, M. Wirth, Lectin mediated biorecognition as a novel strategy for targeted delivery to bladder cancer, J. Urol. 186 (4) (2011) 1481–1488.
[23] C. Apfelthaler, M. Anzengruber, F. Gabor, M. Wirth, Poly – (L) – glutamic acid drug delivery system for the intravesical therapy of bladder cancer using WGA as targeting moiety, Eur. J. Pharm. Biopharm. [Internet] 115 (2017) 131–139.
[24] L. Neutsch, B. Eggenreich, E. Herwig, M. Marchetti-Deschmann, G. Allmaier, F. Gabor, M. Wirth, Lectin bioconjugates trigger urothelial cytoinvasion–a glycotargeted approach for improved intravesical drug delivery, Eur. J. Pharm. Biopharm. 82 (2) (2012) 367–375.
[25] L. Neutsch, M. Wambacher, E.-M. Wirth, S. Spijker, H. Kählig, M. Wirth, F. Gabor, UPEC biomimickry at the urothelial barrier: lectin-functionalized PLGA microparticles for improved intravesical chemotherapy, Int. J. Pharm. 450 (1-2) (2013) 163–176.
[26] N. Lochner, F. Pittner, M. Wirth, F. Gabor, Wheat germ agglutinin binds to the epidermal growth factor receptor of artificial Caco-2 membranes as detected by silver nanoparticle enhanced fluorescence, Pharm. Res. 20 (5) (2003) 833–839.
[27] K.S. Suslick, M.W. Grinstaff, K.J. Kolbeck, M. Wong, Characterization of sonochemically prepared proteinaceous microspheres, Ultrason. Sonochem. 1 (1) (1994) S65–S68.
[28] A. Rollett, T. Reiter, A. Ohradanova-Repic, C. Machacek, A. Cavaco-Paulo, H. Stockinger, G.M. Guebitz, HSA nanocapsules functionalized with monoclonal antibodies for targeted drug delivery, Int. J. Pharm. 458 (1) (2013) 1–8.
[29] D.R. Caudwell, J.P.M. Trusler, V. Vesovic, W.A. Wakeham, The viscosity and density of n-dodecane and n-octadecane at pressures up to 200 MPa and temperatures up to 473 K, Int. J. Thermophys. 25 (5) (2004) 1339–1352.
[30] C.E. Storniolo, N. Martínez-Hovelman, M. Martínez-Huélamo, R.M. Lamuela-Raventos, J.J. Moreno, Extra virgin olive oil minor compounds modulate mitogenic action of oleic acid on colon cancer cell line, J. Agric. Food Chem. 67 (41) (2019) 11420–11427.
[31] A. Thomas, Fats and Fatty Oils. Ullmann's Encyclopedia of Industrial Chemistry. 2000. (Major Reference Works).
[32] V. Mohanra, Y. Chen, Nanoparticles – A review, Trop. J. Pharm. Res. 5 (1) (2006) 561–573.
[33] J. Panyam, V. Labhasetwar, Biodegradable nanoparticles for drug and gene delivery to cells and tissue, Adv. Drug Deliv. Rev. 64 (2012) 61–71.
[34] P. Khandelwal, S.N. Abraham, G. Apodaca, Cell biology and physiology of the uroepithelium, Am. J. Physiol. Renal Physiol. 297 (6) (2009) F1477–F1501.

[35] S.A. Lewis, Everything you wanted to know about the bladder epithelium but were afraid to ask, Am. J. Physiol. Renal Physiol. 278 (6) (2000) F867–F874.
[36] J.P.B. Gasión, J.F.J. Cruz, Improving efficacy of intravesical chemotherapy, Eur. Urol. 50 (2) (2006) 225–234.
[37] D. Chiumello, F. Tallarini, M. Chierichetti, F. Polli, G. Li Bassi, G. Motta, S. Azzari, C. Carsenzola, L. Gattinoni, The effect of different volumes and temperatures of saline on the bladder pressure measurement in critically ill patients, Crit. Care 11 (4) (2007) R82.